

Closed-loop Analysis of Vision-based Autonomous Systems: A Case Study

Corina Păsăreanu^{1,2}, Ravi Mangal², Divya Gopinath¹, Sinem Getir Yaman³,
Calum Imrie³, Radu Călinescu³, and Huafeng Yu⁴

¹ KBR, NASA Ames, Moffett Field CA 94035, USA

² Carnegie Mellon University, Moffett Field CA 94035, USA

³ University of York, York, UK

⁴ Boeing Research and Technology, Santa Clara, CA

Abstract. Deep neural networks (DNNs) are increasingly used in safety-critical autonomous systems as perception components processing high-dimensional image data. Formal analysis of these systems is particularly challenging due to the complexity of the perception DNNs, the sensors (cameras), and the environment conditions. We present a case study applying formal probabilistic analysis techniques to an experimental autonomous system that guides airplanes on taxiways using a perception DNN. We address the above challenges by replacing the camera and the network with a compact probabilistic abstraction built from the confusion matrices computed for the DNN on a representative image data set. We also show how to leverage local, DNN-specific analyses as run-time guards to increase the safety of the overall system. Our findings are applicable to other autonomous systems that use complex DNNs for perception.

1 Introduction

Complex autonomous systems, such as autonomous aircraft taxiing systems [31] and autonomous cars [19, 40, 25], need to perceive and reason about their environments using high-dimensional data streams (such as images) generated by rich sensors (such as cameras). Machine learnt components, specially deep neural networks (DNNs), are particularly capable of the required high-dimensional reasoning and hence, are increasingly used for perception in these systems. While formal analysis of the safety of these systems is highly desirable due to their safety-critical operational settings and the error-prone nature of learned components, in practice this is very challenging because of the complexity of the system components, including the high complexity of the neural networks (which may have thousands or millions of parameters), the complexity of the high-definition cameras that are used to capture the images, and the complexity of the environment in which the system operates (i.e., the world itself).

In this work, we describe a formal analysis of a closed-loop autonomous system that addresses the above challenges. Our case study is motivated by a real-world application, namely, an experimental autonomous system for guiding airplanes on taxiways developed by Boeing [2, 13].

The key idea is to abstract away altogether the perception components, namely, the perception network and the image generator, i.e., the camera taking images of the world, and replace them with a probabilistic component α that maps (abstractions of) the state of the world to state estimates that are used in downstream decision making in the closed-loop system. The resulting system can then be analyzed with standard (probabilistic) model checkers, such as PRISM [34] or STORM [22].

The approach is *compositional*, in the sense that the probabilistic component is computed separately from the rest of the system. The transition probabilities in α are derived based on *confusion matrices* computed for the DNN (measured on representative data sets). Developers routinely use confusion matrices to evaluate machine learning models, so our analysis is closely aligned with existing work-flows, facilitating its adoption in practice.

The size of the probabilistic abstraction α is linear in the size of the output of the DNN, and is independent of the number of the DNN parameters or the complexity of the camera and the environment. We also describe how to leverage additional results obtained from analyzing the DNN in isolation (using DNN-specific methods [16, 26, 17, 20, 32, 35]) to further refine the abstraction and also increase the safety of the closed-loop system through *run-time guards*.

The probabilities in α are estimated based on empirical data, so they are subject to error. We explore the use of *confidence intervals* in addition to point estimates for these probabilities and thereby strengthen the soundness of the analysis [4, 6]. We also leverage rules mined from the DNN model [16] to act as run-time guards for the closed-loop analysis, thereby demonstrating its application in a realistic setting. Our technique is applicable to other autonomous systems that use DNN-based perception from high-dimensional data.

Related Work. Formal proofs of closed-loop safety have been obtained for systems with low-dimensional sensor readings [38, 29, 30, 28, 27, 11, 10]; however, they become intractable for systems that use rich sensors producing high-dimensional inputs such as images.

Other works address the modeling and scalability challenges by constructing *abstractions* of the perception components [24, 33]. To model different environment conditions, these abstract models use *non-deterministic* transitions. The resulting closed-loop systems are analyzed with traditional (non-probabilistic) techniques. The abstractions either lack soundness proofs [33] or come with only probabilistic soundness guarantees [24] which do not translate into probabilistic guarantees over the safety of the overall system. VerifAI [15] can find counter-examples to system safety, but can not provide guarantees.

In contrast to previous work, we describe a formal analysis that is *probabilistic*, which we believe is natural since the camera images capturing the state of the world are subject to randomness due to the environment; further DNNs are learnt from data and are not guaranteed to be 100% accurate. We build on our previous work DEEPDECS [5], where the goal is to perform controller synthesis with safety guarantees, so the formalism is more involved. Furthermore, DEEPDECS does not consider confidence interval analysis, which we explore here based on

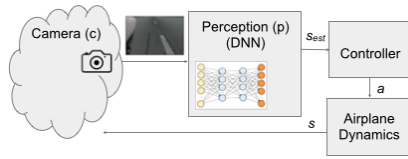


Fig. 1: Closed-loop System

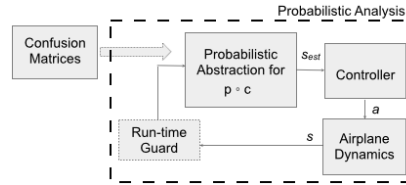


Fig. 2: Abstracted System

some of our other previous works [4, 6]. We analyzed center-line tracking using TaxiNet in [31]. That work focuses on the analysis of the network and not on the overall system.

2 Autonomous Center-line Tracking with TaxiNet

Boeing is developing an experimental autonomous system for center-line tracking on taxiways in an airport. The system uses a neural network called TaxiNet for perception. TaxiNet is designed to take a picture of the taxiway as input and return the plane’s position with respect to the center-line on the taxiway. It returns two outputs; cross track error (**cte**), which is the distance in meters of the plane from the center-line and heading error (**he**), which is the angle in degrees of the plane with respect to the center-line. These outputs are fed to a controller which in turn manoeuvres the plane such that it remains close to the center of the taxiway. This forms a closed-loop system where the perception network continuously receives images as the plane moves on the taxiway. We use this system as a case study and also as a running example throughout the paper.

System Decomposition. The decomposition of this system is illustrated in Figure 1. The controller sends actions a to the airplane to guide it on the taxiway. The dynamics (which models the movement of the airplane on the airport surface) maps previous state s and action a to the next state s' .¹ Information about the taxiway is provided by the perception network (p), i.e. TaxiNet. The perception network takes high-dimensional images captured with a *camera* (c), and returns its estimation s_{est} of the real state s .

For our application, state $s \in S$ captures the position of the airplane on the surface; S is modeled as $\text{CTE} \times \text{HE}$. The network estimates the state $s := (\text{cte}, \text{he})$ based on images taken with a camera placed on the airplane. If the network is ‘perfect’, then $s = s_{est}$.² However, this does not hold in practice. The network is trained on a finite set of images and is not guaranteed to be 100% accurate whereas images observed in operation show a wide variety due to different environment (e.g., light, weather) conditions and imperfections in the camera.

Component Modeling. We built a simple discrete model of the airplane dynamics and a discrete-time controller for the system, similar to previous related work [23, 3] which also considers discretized control. Since the controller is

¹ Velocity may be provided as feedback to the controller; we ignore here for simplicity.

² Assuming the relevant state of the world is recoverable from the input image.

discretized, we abstract the regression outputs of TaxiNet to view the model as a classifier which predicts the plane’s position in discrete states. Treatment of more complex systems with continuous semantics and regression models is left for future work. The main challenge that we address in the paper is the modeling of the perception components (the camera and the network), which we describe in detail in the next section. We model the (abstracted) autonomous system as a Discrete Time Markov Chain (DTMC) [36]; the code is shown in the appendix.

Safety Properties. In our study, the goal is to provide *guarantees* for safe behaviour with respect to two system-level properties indicated by our industrial partner. The properties specify conditions for safe operation in terms of allowed `cte` and `he` values for the airplane, by using taxiway dimensions. The first property states that the airplane shall never leave the taxiway (i.e., $|\text{cte}| \leq 8$ meters). The second property states that the airplane shall never turn more than a prescribed degree (i.e., $|\text{he}| \leq 35$ degrees), as it would be difficult to maneuver the airplane from that position. We encode the two properties in PCTL [7] as follows.

$$P =?[F(\text{cte} = -1)] \quad (\textit{Property 1})$$

$$P =?[F(\text{he} = -1)] \quad (\textit{Property 2})$$

Here “-1” denotes an error for either `cte` or `he` (meaning that the airplane is either off the taxiway or turned more than the prescribed angle) and $P =?$ indicates that we want to calculate the probability that eventually (F) the system reaches an error state.

3 Probabilistic Analysis

In this section, we describe the methodology for abstracting and analyzing an autonomous system leveraging probabilistic model checking. The main idea, which we initially explored in [5], is to replace the composition $p \circ c$ of the camera (denoted as c) and the perception DNN (denoted as p) with a probabilistic map $\alpha : S \rightarrow \mathcal{D}(S)$ from system states to a discrete distribution over system states. Figure 2 depicts the abstracted autonomous system.

We observe that c can be viewed as a map between state $s \in S$ to a distribution over images, denoted as $\mathcal{D}(\text{Img})$, where $\text{img} \in \text{Img}$ and Img is the set of images. For instance, in the TaxiNet system, state s only captures the position of the airplane with respect to the center-line, but there are many different images that correspond to the same position. This is due to uncontrollable environmental conditions, such as temporary sensor failures or different lighting and weather conditions. Consequently, a single state s can map to a number of different images depending on the environment, and this is modeled by considering c to be a probabilistic map of type $S \rightarrow \mathcal{D}(\text{Img})$. Given a system state s , $\alpha(s)$ models the probability of $p \circ c$ leading to a particular estimated state s_{est} ; α needs to be probabilistic because c itself is probabilistic and p is not perfectly accurate. The probabilities can be empirically estimated via a confusion matrix that records the performance of the network on a *representative* data set.

We further describe how we can leverage DNN-specific analysis to improve the accuracy of perception and the safety of the overall system, via the optional addition of run-time guards. For the verification of the closed-loop system, we use the PRISM model checking tool [34]. We also explore methods for analysis of DTMCs with uncertain transition probabilities [4, 6], to obtain *probabilistic guarantees* about the validity of our probabilistic safety proofs even though the abstraction probabilities are empirical estimates.

Assumptions. Our analysis assumes that the distribution of inputs to the network remains fixed over time (i.e., it is not subject to distribution shifts). Moreover, the data set of input images used to estimate the probabilities in α is assumed to be *representative*, i.e., constituted of independently drawn samples from this fixed underlying distribution of inputs. Relaxing these assumptions is a challenging but important task for future research.

3.1 Probabilistic Abstractions for Perception

We describe in detail the construction of the probabilistic abstraction $\alpha : S \rightarrow \mathcal{D}(S)$. We do not need access to the camera and only require black-box access to the network for constructing our abstraction.³ We assume S is a finite set such that $\#S = K$ where $\#S$ denotes the cardinality of set S . We use $\alpha(s, s_{est})$ to represent the probability associated with estimated state s_{est} . It is defined as,

$$\alpha(s, s_{est}) := \Pr_{\text{img} \sim c(s)} [p(\text{img}) = s_{est}] \quad (1)$$

We estimate the probabilities in α by means of a confusion matrix. Let $\overline{\text{Img}}_s \subseteq \text{Img}$ denote a *representative test dataset* for images corresponding to state s , i.e., every sample in $\overline{\text{Img}}_s$ is assumed to be an independently drawn sample from $c(s)$. We assume access to representative test datasets corresponding to every state $s \in S$. Let $\overline{\text{Img}} := \bigcup_{s \in S} \overline{\text{Img}}_s$. For any test input $\text{img} \in \overline{\text{Img}}$, let $p^*(\text{img}) \in S$ be the label (i.e., the true underlying state) of img , which is known since $\overline{\text{Img}}$ is a test dataset. For the sake of technical presentation, we assume a bijective map $\text{rep} : S \rightarrow [K]$ that maps every state in S to a number in $[K] := \{1, 2, \dots, K\}$. We evaluate p on the test dataset $\overline{\text{Img}}$ to construct a $K \times K$ confusion matrix \mathcal{C} such that, for any $k, k' \in [K]$, the element in row k and column k' of this matrix is given by the number of inputs from $\overline{\text{Img}}$ with true state $\text{rep}^{-1}(k)$ that the perception network p classifies as state $\text{rep}^{-1}(k')$.

$$\mathcal{C}[k, k'] := \# \{ \text{img} \in \overline{\text{Img}} \mid p^*(\text{img}) = \text{rep}^{-1}(k) \wedge p(\text{img}) = \text{rep}^{-1}(k') \} \quad (2)$$

Given the confusion matrix \mathcal{C} , empirical estimates for the probabilities in α are calculated as follows,

$$\alpha(\text{rep}^{-1}(k), \text{rep}^{-1}(k')) := \frac{\mathcal{C}[k, k']}{\sum_{k'' \in [K]} \mathcal{C}[k, k'']}. \quad (3)$$

³ Our run-time guard does require white-box access.

TaxiNet Example. For the Taxinet application, we construct two probabilistic maps, α_{cte} and α_{he} , corresponding to each of the state variables `cte` and `he`, using a representative test data set with 11108 samples.⁴ Thus, α_{cte} is of type $\text{CTE} \rightarrow \mathcal{D}(\text{CTE})$

and α_{he} is of type $\text{HE} \rightarrow \mathcal{D}(\text{HE})$. Table 1 illustrates the confusion matrix for `he`. The mapping α_{he} is computed in a straightforward way: $\alpha_{he}(0,0) = 4748/(4748 + 2139 + 148) = 0.675$, giving the probability of estimating correctly that the value of `he` is zero. Similarly, $\alpha_{he}(1,0) = 91/(91 + 2010) = 0.043$, giving the probability of estimating incorrectly that the value of `he` is zero instead of one. The corresponding DTMC code is as follows:

		Predicted		
		0	1	2
Actual	0	4748	2139	148
	1	91	2010	0
	2	744	211	1017

Table 1: Confusion Matrix for `he`

```

[] he=0 → 0.675: (he_est'=0) + 0.304: (he_est'=1) + 0.021: (he_est'=2);
[] he=1 → 0.043: (he_est'=0) + 0.957: (he_est'=1) + 0.0: (he_est'=2);
[] he=2 → 0.377: (he_est'=0) + 0.107: (he_est'=1) + 0.516: (he_est'=2);

```

A similar computation is performed for constructing α_{cte} . The resulting code for the closed-loop system is shown in Appendix B.1.

3.2 DNN Checks as Run-Time Guards

We use DNN-specific checks as run-time guards to improve the performance of the perception network and therefore the safety of the overall system. We hypothesize that for inputs where the checks pass, the network is more likely to be accurate, and therefore, the system is safer.

For our case study, we extract input-output rules from the DNN and use them as run-time guards (as described in Section 4). More generally, one can use any off-the-shelf pointwise DNN check, such as local robustness [18, 37, 39, 9, 14, 35] or confidence checks for well-calibrated networks [20], as run-time guards (provided that they are fast enough to be deployed in practice). For practical reasons (TaxiNet is a regression model, it contains ELU [8] activations, we do not have access to the training data) we can not use off-the-shelf checks here.

Modeling DNN Checks. Let us denote the application of (one or more) DNN-specific checks as a function $\text{check} : (\text{Img} \rightarrow S) \times \text{Img} \rightarrow \mathbb{B}$, such that, for perception network $p \in \text{Img} \rightarrow S$ and image $\text{img} \in \text{Img}$, $\text{check}(p, \text{img}) = \text{true}$ if p passes the checks at input img , and $\text{check}(p, \text{img}) = \text{false}$ otherwise.

We further assume that a system that uses DNN checks as a run-time guard attempts to read the camera sensor multiple (one or more) times, until the check passes; and aborts (or goes to a fail-safe state) if the number of consecutive failed checks reaches a certain threshold. This logic can be generalized to consider more sophisticated safe-mode operations; for instance, the system can decelerate and/or notify an operator when the threshold is reached, as this could indicate serious sensor failure or adverse weather conditions.

⁴ To simplify the DTMCs, we model the updates to `cte` and `he` as independent. For more precision, we can compute confusion matrices and α for the pair (cte, he) .

To model the effect of the run-time check in our analysis, we can define β as the probability that an image img generated by the camera c , for *any* state s , satisfies $\text{check}(p, \text{img}) = \text{true}$;

$$\beta := \Pr_{\text{img} \sim D} [\text{check}(p, \text{img}) = \text{true}] \quad (4)$$

Here D is the distribution obtained by *combining* $c(s)$ for all states $s \in S$.⁵ To be more precise we can define a separate β_s for each state s . We estimate β using the representative set of images $\overline{\text{Img}}$,

$$\beta := \frac{\#\overline{\text{Img}}^{\text{true}}}{\#\overline{\text{Img}}} \quad (5)$$

where $\overline{\text{Img}}^{\text{true}} := \{\text{img} \in \overline{\text{Img}} \mid \text{check}(p, \text{img}) = \text{true}\}$.

For the overall analysis of the closed-loop system, irrespective of the state s , we can assume that the DNN check will pass with a probability β . Moreover, since the perception network only processes images that pass the DNN check, we construct a refined probabilistic abstraction α^{true} using conditional probability:

$$\alpha^{\text{true}}(s, s_{\text{est}}) := \Pr_{\text{img} \sim c(s)} [p(\text{img}) = s_{\text{est}} \mid \text{check}(p, \text{img}) = \text{true}] \quad (6)$$

We can estimate α^{true} as before, but the confusion matrix is built using only the images that pass the DNN check, i.e., for dataset $\overline{\text{Img}}^{\text{true}} \subseteq \overline{\text{Img}}$.

TaxiNet Example. For TaxiNet, out of 11108 inputs, 9125 inputs (i.e., 82.1%) pass the DNN check resulting in the following code:

```
i:[0..M] init 0;
[] pc=0 & i<M → 0.821: (v'=1) & (pc'=1) & (i'=0) + 0.179: (v'=0) & (i'=i+1);
```

We model the result of applying the DNN check with variable v ; $v = 1$ if the check returns **true** for an image and $v = 0$ otherwise. M is the number of allowed repeated sensor readings and i is used to count the number of failed DNN checks.

The abstraction for state variables he (α_{he}) and cte (α_{cte}) is only computed for the inputs that pass the check (i.e., for $v = 1$) based on newly computed confusion matrices. The DTMC code for the closed-loop system with run-time guards is in Appendix B.2.

3.3 Confidence Analysis

The construction of the probabilistic abstractions relies on calculating empirical point estimates of the required probabilities. However, these empirical estimates lack statistical guarantees and can be off by an arbitrary amount from the true probabilities. To address this concern, we experiment with using FACT [4, 6] to calculate *confidence intervals* for the probability that the safety properties of the closed-loop system are satisfied. The inputs to FACT are: 1) a parametric

⁵ To simplify the presentation, we omit the precise mathematical formulation for D .

DTMC m where each empirically estimated transition probability is represented by a parameter, 2) a PCTL formula ϕ , 3) an error level $\delta \in (0, 1)$ and 4) an *observation function* O mapping state s to a tuple representing the number of observations for each outgoing transition from s ; in our case, the number of observations can be obtained directly from the computed confusion matrices, i.e., $O(s) = (\mathcal{C}[\text{rep}(s), 1], \dots, \mathcal{C}[\text{rep}(s), K])$. FACT synthesizes a $(1 - \delta)$ -confidence interval $[a, b] \subseteq [0, 1]$ for the probability that ϕ is satisfied, given the observations.

Taxinet Example. The following partial code illustrates the parametric version of the code provided in Section 3.1 (with the complete code for the parametric models provided in Appendix C). The first three lines represent the number of observations obtained from the confusion matrix in Table 1.

```

param double x = 4748 2139 148;
param double y = 91 2010;
param double z = 744 211 1017;
...
[] he=0 → x1:(he_est'=0) + x2:(he_est'=1) + (1-x1-x2):(he_est'=2);
[] he=1 → y1:(he_est'=0) + (1-y1):(he_est'=1);
[] he=2 → z1:(he_est'=0) + z2:(he_est'=1) + (1-z1-z2):(he_est'=2);

```

4 Experiments

In this section, we report on the experiments that we conducted as part of our probabilistic safety analysis of the center-line tracking autonomous system.

We built two DTMC models, m_1 and m_2 , denoting the closed-loop center-line tracking system without and with a run-time guard, respectively. The airplane dynamics and the controller are identically modeled in the two DTMCs as discrete components. The code for the models (in PRISM syntax) and more details about the analysis are presented in the appendix.

TaxiNet DNN. This is a regression model with 24 layers including five convolution layers, and three dense layers (with 100/50/10 ELU neurons) before the output layer. The inputs to the model are RGB color images of size 360×200 pixels. We use a representative data set with 11108 images, shared by our industry partner. The model has a Mean Absolute Error (MAE) of 1.185 for **cte** and 7.86 for **he** outputs respectively. The discrete nature of the controller in our DTMCs induces a discretization on TaxiNet’s outputs and the treatment of TaxiNet as a classifier for the purpose of our analysis. The **cte** $\in [-8.0 \text{ m}, 8.0 \text{ m}]$ and **he** $\in [-35.0^\circ, 35.0^\circ]$ outputs of the regression model are translated into classifier outputs $\underline{\text{cte}} \in \{0, 1, 2, 3, 4\}$ and $\underline{\text{he}} \in \{0, 1, 2\}$ as shown below.

$$\underline{\text{cte}} = \begin{cases} 3 & \text{if } -8.0 \text{ m} \leq \text{cte} \leq -4.8 \text{ m} \\ 1 & \text{if } -4.8 \text{ m} \leq \text{cte} \leq -1.6 \text{ m} \\ 0 & \text{if } -1.6 \text{ m} \leq \text{cte} \leq 1.6 \text{ m} \\ 2 & \text{if } 1.6 \text{ m} \leq \text{cte} \leq 4.8 \text{ m} \\ 4 & \text{if } 4.8 \text{ m} \leq \text{cte} \leq 8.0 \text{ m} \end{cases} \quad \underline{\text{he}} = \begin{cases} 1 & \text{if } -35.0^\circ \leq \text{he} \leq -11.67^\circ \\ 0 & \text{if } -11.67^\circ \leq \text{he} \leq 11.66^\circ \\ 2 & \text{if } 11.66^\circ \leq \text{he} \leq 35.0^\circ \end{cases}$$

We use label “-1” to denote error states, i.e., $\underline{\text{cte}} = -1$ iff $|\text{cte}| > 8 \text{ m}$ and $\underline{\text{he}} = -1$ iff $|\text{he}| > 35^\circ$. For simplicity, we use **cte** and **he** to denote both the

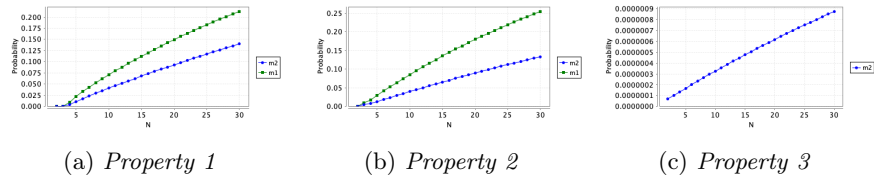


Fig. 3: Probabilistic model checking results via PRISM

classifier and regression outputs in other parts of the paper (with meaning clear from context). Note that none of the input images are labeled by the classifier as “-1”; however, this does not preclude the system from reaching an error.

Mining Rules for Run-time Guards. We leverage our prior work [16], to extract rules of the form $Pre \implies Post$ from the DNN. $Post$ is the condition $|\text{cte}^* - \text{cte}| > 1.0 \text{ m} \vee |\text{he}^* - \text{he}| > 5^\circ$ on the regression model’s outputs and Pre is a condition over the neuron values in the three dense layers of TaxiNet (cte^* and he^* denote ground-truth values). The considered $Post$ characterizes model misbehavior (as explained in [31]). If an input satisfies Pre , the DNN check is considered to have failed on that input. Pre can be evaluated efficiently during the forward pass of the model, making it a good run-time guard candidate. More details on the rules are in Appendix D.

Confusion Matrices. The confusion matrices for the classification version of TaxiNet, computed for the two cases (without and with run-time guard) are shown in Tables 2 and 3 in Appendix A. The tables can be used by developers to better understand the DNN performance. For instance, the DNN performs best for inputs lying on the center-line, which can be attributed to training being done mainly using scenarios where the plane follows the center-line. The model appears to perform better when the plane is heading left, as opposed to heading right, which may be due to camera position. These observations can be used by developers to improve the model, by training on more scenarios. Note also that the model does not make ‘blatant’ errors, mistaking inputs on the *left* as being on the *right* (of center-line) or vice-versa (see e.g., entries with zero observations). Formal proofs can provide guarantees of absence of such transitions.

Analysis. We analyzed m_1 and m_2 with respect to the two PCTL properties, $P = ?[F(\text{cte} = -1)]$ (*Property 1*), and $P = ?[F(\text{he} = -1)]$ (*Property 2*). The airplane is assumed to start from a initial position on the center-line and heading straight. For m_2 , i.e. the model with a run-time guard, we also evaluate the probability of the TaxiNet system going to the abort state using the property, $P = ?[F(v = 0 \ \& \ i = M)]$ (*Property 3*), where M is the threshold for the number of consecutive run-time check failures.

The probabilities of these properties being satisfied, calculated by PRISM, are shown in Figure 3, where N is a constant in the DTMCs that dictates the length of the finite-time horizon considered for the analysis. The confidence intervals computed with FACT are shown in Figure 4, at different confidence levels (0.95 to 0.99), for $N = 4$. For computing the intervals, we ignore the transitions in the DTMCs that were not observed in our data (see Appendix E for more details).

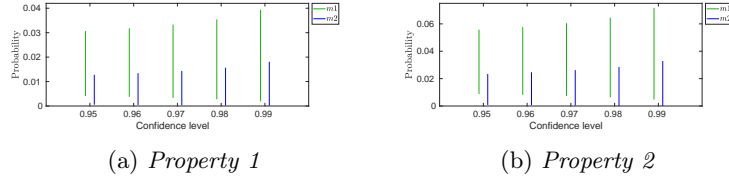


Fig. 4: Confidence interval results via FACT

The PRISM analysis scales well; e.g., evaluating *Property 1* for model m_2 ($N = 30$) requires less than 0.1 seconds on an M1 MacBook Pro, 16 GB RAM. The numbers are similar for other queries. However, the confidence analysis does not scale as well; we could not go beyond $N = 4$ for a timeout of two hours, with *Property 1* hardest to check. Newer work, fPMC [12], addresses these scalability challenges but we found it not yet mature enough to be applied to our models.

Discussion and Lessons Learned. The experiments demonstrate the feasibility of our approach, which enables reasoning about a complex DNN interacting with conventional (discrete-time) components via a simple probabilistic abstraction. Our analysis not only provides qualitative (i.e., an error is reachable or not) but also quantitative (i.e., likelihood of error) results, helping developers assess the risk associated with the analyzed scenario.

The results highlight the benefit of the run-time guards in improving the safety of the overall system; see Figures 3(a,b) for lower error probabilities and Figures 4(a,b) for tighter intervals for m_2 . The probability of aborting is very small, indicating the efficacy of the fail-safe mechanism (see Figures 3(c),6). More importantly, since the DNN demonstrates higher accuracy on the inputs where the run-time check passes, the results also indicate that *improved accuracy of the DNN translates into improved safety*. The computed probabilities and confidence intervals can be examined by developers and regulators to ensure that system safety is met at required levels. If the confidence intervals are too large, they can be made tighter by adding more data, as guided by the confusion matrices.

5 Conclusion

We demonstrated a method for the analysis of the safety of autonomous systems that use complex DNNs for visual perception. Our abstraction helps separate the concerns of DNN and conventional system development and evaluation. It also enables the integration of heterogeneous artifacts from DNN-specific analysis and system-level probabilistic model checking. The approach produces not only qualitative results but also provides insights that can be used in quantitative safety assessment for AI/DNN-enabled systems. This is, potentially, an important step to fill one of the gaps of quantitative evaluation for future AI certification [1].

Future work involves more experimentation with image data sets representing a wide variety of environment conditions. We also plan to refine our models, inducing finer partitions on the DNN, and validate them through hardware simulations. Finally, we plan to study the composition of safety proofs for the system analyzed in different scenarios.

References

1. EASA concept paper: First usable guidance for level 1 machine learning applications (2021), <https://www.easa.europa.eu/en/downloads/134357/en>
2. Beland, S., Chang, I., Chen, A., Moser, M., Paunicka, J.L., Stuart, D., Vian, J., Westover, C., Yu, H.: Towards assurance evaluation of autonomous systems. In: IEEE/ACM International Conference On Computer Aided Design, ICCAD 2020, San Diego, CA, USA, November 2-5, 2020. pp. 84:1–84:6. IEEE (2020)
3. Byrne, R., Abdallah, C., Dorato, P.: Experimental results in robust lateral control of highway vehicles. In: Proceedings of 1995 34th IEEE Conference on Decision and Control. vol. 4, pp. 3572–3575 vol.4 (1995)
4. Calinescu, R., Ghezzi, C., Johnson, K., Pezzé, M., Rafiq, Y., Tamburrelli, G.: Formal verification with confidence intervals to establish quality of service properties of software systems. *IEEE transactions on reliability* **65**(1), 107–125 (2015)
5. Calinescu, R., Imrie, C., Mangal, R., Păsăreanu, C., Santana, M.A., Vázquez, G.: Discrete-event controller synthesis for autonomous systems with deep-learning perception components. *arXiv preprint arXiv:2202.03360* (2022)
6. Calinescu, R., Johnson, K., Paterson, C.: Fact: A probabilistic model checker for formal verification with confidence intervals. In: International Conference on Tools and Algorithms for the Construction and Analysis of Systems. pp. 540–546. Springer (2016)
7. Ciesinski, F., Größer, M.: On Probabilistic Computation Tree Logic, pp. 147–188. Springer Berlin Heidelberg (2004)
8. Clevert, D.A., Unterthiner, T., Hochreiter, S.: Fast and accurate deep network learning by exponential linear units (elus). *arXiv preprint arXiv:1511.07289* (2015)
9. Cohen, J., Rosenfeld, E., Kolter, Z.: Certified adversarial robustness via randomized smoothing. In: Chaudhuri, K., Salakhutdinov, R. (eds.) Proceedings of the 36th International Conference on Machine Learning. Proceedings of Machine Learning Research, vol. 97, pp. 1310–1320. PMLR (09–15 Jun 2019)
10. Dawson, C., Gao, S., Fan, C.: Safe control with learned certificates: A survey of neural lyapunov, barrier, and contraction methods. *arXiv preprint arXiv:2202.11762* (2022)
11. Dawson, C., Lowenkamp, B., Goff, D., Fan, C.: Learning safe, generalizable perception-based hybrid control with certificates. *IEEE Robotics and Automation Letters* **7**(2), 1904–1911 (2022)
12. Fang, X., Calinescu, R., Gerasimou, S., Alhwikem, F.: Software performability analysis using fast parametric model checking (2022)
13. Frew, E., McGee, T., Kim, Z., Xiao, X., Jackson, S., Morimoto, M., Rathinam, S., Padiyal, J., Sengupta, R.: Vision-based road-following using a small autonomous aircraft. In: 2004 IEEE Aerospace Conference Proceedings (IEEE Cat. No.04TH8720). vol. 5, pp. 3006–3015 Vol.5 (2004)
14. Fromherz, A., Leino, K., Fredrikson, M., Parno, B., Pasareanu, C.: Fast geometric projections for local robustness certification. In: International Conference on Learning Representations (2021)
15. Ghosh, S., Pant, Y.V., Ravanbakhsh, H., Seshia, S.A.: Counterexample-guided synthesis of perception models and control. In: 2021 American Control Conference (ACC). pp. 3447–3454. IEEE (2021)
16. Gopinath, D., Converse, H., Pasareanu, C., Taly, A.: Property inference for deep neural networks. In: International Conference on Automated Software Engineering (ASE). pp. 797–809. IEEE (2019)

17. Gopinath, D., Katz, G., Pasareanu, C.S., Barrett, C.W.: Deepsafe: A data-driven approach for checking adversarial robustness in neural networks. CoRR **abs/1710.00486** (2017)
18. Gowal, S., Dvijotham, K., Stanforth, R., Bunel, R., Qin, C., Uesato, J., Arandjelovic, R., Mann, T., Kohli, P.: On the effectiveness of interval bound propagation for training verifiably robust models. arXiv preprint arXiv:1810.12715 (2018)
19. Grigorescu, S.M., Trasnea, B., Cocias, T.T., Macesanu, G.: A survey of deep learning techniques for autonomous driving. CoRR **abs/1910.07738** (2019)
20. Guo, C., Pleiss, G., Sun, Y., Weinberger, K.Q.: On calibration of modern neural networks. CoRR **abs/1706.04599** (2017)
21. Gurobi Optimization, LLC: Gurobi Optimizer Reference Manual (2023), <https://www.gurobi.com>
22. Hensel, C., Junges, S., Katoen, J.P., Quatmann, T., Volk, M.: The probabilistic model checker Storm. International Journal on Software Tools for Technology Transfer **24**(4), 589–610 (Aug 2022)
23. Hoffmann, G.M., Tomlin, C.J., Montemerlo, M., Thrun, S.: Autonomous automobile trajectory tracking for off-road driving: Controller design, experimental validation and racing. In: American Control Conference, ACC 2007, New York, NY, USA, 9-13 July, 2007. pp. 2296–2301. IEEE (2007)
24. Hsieh, C., Li, Y., Sun, D., Joshi, K., Misailovic, S., Mitra, S.: Verifying controllers with vision-based perception using safe approximate abstractions. IEEE Transactions on Computer-Aided Design of Integrated Circuits and Systems **41**(11), 4205–4216 (2022)
25. Huang, X., Kroening, D., Ruan, W., Sharp, J., Sun, Y., Thamo, E., Wu, M., Yi, X.: A survey of safety and trustworthiness of deep neural networks: Verification, testing, adversarial attack and defence, and interpretability. Computer Science Review **37**, 100270 (2020)
26. Huang, X., Kwiatkowska, M., Wang, S., Wu, M.: Safety verification of deep neural networks. CoRR **abs/1610.06940** (2016)
27. Ivanov, R., Carpenter, T., Weimer, J., Alur, R., Pappas, G., Lee, I.: Verisig 2.0: Verification of neural network controllers using taylor model preconditioning. In: International Conference on Computer Aided Verification. pp. 249–262. Springer (2021)
28. Ivanov, R., Carpenter, T.J., Weimer, J., Alur, R., Pappas, G.J., Lee, I.: Verifying the safety of autonomous systems with neural network controllers. ACM Transactions on Embedded Computing Systems (TECS) **20**(1), 1–26 (2020)
29. Ivanov, R., Jothimurugan, K., Hsu, S., Vaidya, S., Alur, R., Bastani, O.: Compositional learning and verification of neural network controllers. ACM Transactions on Embedded Computing Systems (TECS) **20**(5s), 1–26 (2021)
30. Ivanov, R., Weimer, J., Alur, R., Pappas, G.J., Lee, I.: Verisig: verifying safety properties of hybrid systems with neural network controllers. In: Proceedings of the 22nd ACM International Conference on Hybrid Systems: Computation and Control. pp. 169–178 (2019)
31. Kadron, I.B., Gopinath, D., Pasareanu, C.S., Yu, H.: Case study: Analysis of autonomous center line tracking neural networks. In: Bloem, R., Dimitrova, R., Fan, C., Sharygina, N. (eds.) Software Verification - 13th International Conference, VSTTE 2021, New Haven, CT, USA, October 18-19, 2021, and 14th International Workshop, NSV 2021, Los Angeles, CA, USA, July 18-19, 2021, Revised Selected Papers. pp. 104–121. Lecture Notes in Computer Science (2021)

32. Katz, G., Huang, D.A., Ibeling, D., Julian, K., Lazarus, C., Lim, R., Shah, P., Thakoor, S., Wu, H., Zeljic, A., Dill, D.L., Kochenderfer, M.J., Barrett, C.W.: The marabou framework for verification and analysis of deep neural networks. In: Computer Aided Verification - 31st International Conference, CAV 2019, New York City, NY, USA, July 15-18, 2019, Proceedings, Part I. pp. 443–452 (2019)
33. Katz, S.M., Corso, A.L., Strong, C.A., Kochenderfer, M.J.: Verification of image-based neural network controllers using generative models. *Journal of Aerospace Information Systems* **19**(9), 574–584 (2022)
34. Kwiatkowska, M., Norman, G., Parker, D.: PRISM 4.0: Verification of probabilistic real-time systems. In: Gopalakrishnan, G., Qadeer, S. (eds.) Proc. 23rd International Conference on Computer Aided Verification (CAV'11). LNCS, vol. 6806, pp. 585–591. Springer (2011)
35. Leino, K., Wang, Z., Fredrikson, M.: Globally-robust neural networks. In: International Conference on Machine Learning (ICML) (2021)
36. Privault, N.: Discrete-time markov chains, pp. 77–94. Springer Berlin Heidelberg (2013)
37. Raghunathan, A., Steinhardt, J., Liang, P.: Certified defenses against adversarial examples. In: International Conference on Learning Representations (2018)
38. Santa Cruz, U., Shoukry, Y.: Nlander-verif: A neural network formal verification framework for vision-based autonomous aircraft landing. In: NASA Formal Methods Symposium. pp. 213–230. Springer (2022)
39. Singh, G., Gehr, T., Püschel, M., Vechev, M.: An abstract domain for certifying neural networks. *Proceedings of the ACM on Programming Languages* **3**(POPL), 1–30 (2019)
40. Tabernik, D., Skocaj, D.: Deep learning for large-scale traffic-sign detection and recognition. *CoRR* **abs/1904.00649** (2019)

A Confusion Matrices and Transition Probabilities

Accuracy	Grd Truth Label	Tot # inputs	Actual Label	# inputs	Tr Prob
cte (62.39%)	3	398	3	101	0.254
			1	145	0.364
			0	152	0.382
			2	0	0.0
			4	0	0.0
	1	2693	3	11	0.004
			1	992	0.368
			0	1686	0.627
			2	4	0.001
			4	0	0.0
	0	4084	3	0	0.0
			1	40	0.01
			0	3440	0.842
			2	604	0.148
			4	0	0.0
	2	3304	3	0	0.0
			1	4	0.001
			0	1119	0.339
			2	2173	0.658
			4	8	0.002
4	629	3	0	0.0	
		1	0	0.0	
		0	151	0.24	
		2	254	0.404	
		4	224	0.356	
he (69.99%)	1	2101	1	2010	0.957
			0	91	0.043
			2	0	0.0
	0	7035	1	2139	0.304
			0	4748	0.675
			2	148	0.021
	2	1972	1	211	0.107
			0	744	0.377
			2	1017	0.516

Table 2: Results computed on TaxiNet for 11108 inputs.

Accuracy	Grd Truth Label	Tot # inputs	Actual Label	# inputs	Tr Prob
cte (65.78%)	3	330	3	100	0.303
			1	126	0.382
			0	104	0.315
			2	0	0.0
			4	0	0.0
	1	2168	3	11	0.005
			1	951	0.439
			0	1206	0.556
			2	0	0.0
			4	0	0.0
	0	3185	3	0	0.0
			1	32	0.01
			0	2984	0.909
			2	259	0.081
			4	0	0.0
	2	2897	3	0	0.0
			1	2	0.001
			0	1069	0.369
			2	1820	0.628
			4	6	0.002
4	514	3	0	0.0	
		1	0	0.0	
		0	119	0.232	
		2	178	0.346	
		4	217	0.422	
he (76%)	1	1991	1	1902	0.955
			0	89	0.045
			2	0	0.0
	0	5538	1	1388	0.25
			0	4025	0.727
			2	125	0.023
	2	1596	1	76	0.048
0			512	0.32	
			2	1008	0.632

Table 3: Results for TaxiNet, on inputs that pass the DNN check (9125 out of 11108).

B Non-parametric DTMC models for PRISM

B.1 Model m_1 (no run-time guard; $v = 1$ always)

```

1 dtmc
2
3 const N;
4
5 module taxinet
6
7     cte : [-1..4] init 0; //0:center, 1,3:left, 2,4:right, -1:error
8     he : [-1..2] init 0; //0:no angle, 1:negative, 2:positive, -1:error
9     v : [0..1] init 1; //1:certified, 0:not certified
10    cte_est: [0..4] init 0;
11    he_est: [0..2] init 0;
12    a: [0 .. 2] init 0; //0:go straight, 1:turn left, 2: turn right
13    pc:[0..5] init 0; // program counter
14    k:[1..N] init 1; // steps
15
16    // run-time guard: assume we can certify all inputs
17    [] pc=0 → 1: (v'=1) & (pc'=1);
18
19    // NN imperfect perception
20    [] cte=0 & v=1 & pc=1 → 0.842: (cte_est'=0) & (pc'=2) +
21        0.01: (cte_est'=1) & (pc'=2) +
22        0.148: (cte_est'=2) & (pc'=2) +
23        0.0: (cte_est'=3) & (pc'=2) +
24        0.0: (cte_est'=4) & (pc'=2);
25    [] cte=1 & v=1 & pc=1 → 0.627: (cte_est'=0) & (pc'=2) +
26        0.368: (cte_est'=1) & (pc'=2) +
27        0.001: (cte_est'=2) & (pc'=2) +
28        0.004: (cte_est'=3) & (pc'=2) +
29        0.0: (cte_est'=4) & (pc'=2);
30    [] cte=2 & v=1 & pc=1 → 0.339: (cte_est'=0) & (pc'=2) +
31        0.001: (cte_est'=1) & (pc'=2) +
32        0.658: (cte_est'=2) & (pc'=2) +
33        0.0: (cte_est'=3) & (pc'=2) +
34        0.002: (cte_est'=4) & (pc'=2);
35    [] cte=3 & v=1 & pc=1 → 0.382: (cte_est'=0) & (pc'=2) +
36        0.364: (cte_est'=1) & (pc'=2) +
37        0.0: (cte_est'=2) & (pc'=2) +
38        0.254: (cte_est'=3) & (pc'=2) +
39        0.0: (cte_est'=4) & (pc'=2);
40    [] cte=4 & v=1 & pc=1 → 0.24: (cte_est'=0) & (pc'=2) +
41        0.0: (cte_est'=1) & (pc'=2) +
42        0.404: (cte_est'=2) & (pc'=2) +
43        0.0: (cte_est'=3) & (pc'=2) +
44        0.356: (cte_est'=4) & (pc'=2);
45
46
47    [] he=0 & v=1 & pc=2 → 0.675: (he_est'=0) & (pc'=3) +
48        0.304: (he_est'=1) & (pc'=3) +
49        0.021: (he_est'=2) & (pc'=3);
50    [] he=1 & v=1 & pc=2 → 0.043: (he_est'=0) & (pc'=3) +
51        0.957: (he_est'=1) & (pc'=3) +
52        0: (he_est'=2) & (pc'=3);
53    [] he=2 & v=1 & pc=2 → 0.377: (he_est'=0) & (pc'=3) +
54        0.107: (he_est'=1) & (pc'=3) +
55        0.516: (he_est'=2) & (pc'=3);
56
57    //controller:
58    [] cte_est=0 & he_est=0 & pc=3 → 1 : (a'=0) & (pc'=4);
59    [] cte_est=0 & he_est=1 & pc=3 → 1 : (a'=2) & (pc'=4);
60    [] cte_est=0 & he_est=2 & pc=3 → 1 : (a'=1) & (pc'=4);
61
62    [] (cte_est=1 | cte_est=3) & he_est=0 & pc=3 → 1 : (a'=2) & (pc'=4);

```



```

63 [] (cte_est=1 | cte_est=3) & he_est=1 & pc=3 → 1 : (a'=2) & (pc'=4);
64 [] (cte_est=1 | cte_est=3) & he_est=2 & pc=3 → 1 : (a'=0) & (pc'=4);
65
66 [] (cte_est=2 | cte_est=4) & he_est=0 & pc=3 → 1 : (a'=1) & (pc'=4);
67 [] (cte_est=2 | cte_est=4) & he_est=1 & pc=3 → 1 : (a'=0) & (pc'=4);
68 [] (cte_est=2 | cte_est=4) & he_est=2 & pc=3 → 1 : (a'=1) & (pc'=4);
69
70 // airplane dynamics:
71 [] he=1 & a=1 & pc=4 & k<N → 1 : (he'=-1) & (pc'=5); // error
72 [] he=2 & a=2 & pc=4 & k<N → 1 : (he'=-1) & (pc'=5); // error
73
74 [] cte=0 & he=0 & a=0 & pc=4 & k<N → 1 : (pc'=0) & (k'=k+1);
75 [] cte=0 & he=0 & a=1 & pc=4 & k<N → 1 : (cte'=1) & (he'=1) & (pc'=0) &
(k'=k+1);
76 [] cte=0 & he=0 & a=2 & pc=4 & k<N → 1 : (cte'=2) & (he'=2) & (pc'=0) &
(k'=k+1);
77
78 [] cte=0 & he=1 & a=0 & pc=4 & k<N → 1 : (cte'=1) & (pc'=0) & (k'=k+1);
79 [] cte=0 & he=1 & a=2 & pc=4 & k<N → 1 : (he'=0) & (pc'=0) & (k'=k+1);
80
81 [] cte=0 & he=2 & a=0 & pc=4 & k<N → 1 : (cte'=2) & (pc'=0) & (k'=k+1);
82 [] cte=0 & he=2 & a=1 & pc=4 & k<N → 1 : (he'=0) & (pc'=0) & (k'=k+1);
83
84 // left-side dynamics:
85 [] cte=1 & he=0 & a=0 & pc=4 & k<N → 1 : (pc'=0) & (k'=k+1);
86 [] cte=1 & he=0 & a=1 & pc=4 & k<N → 1 : (cte'=3) & (he'=1) & (pc'=0) &
(k'=k+1);
87 [] cte=1 & he=0 & a=2 & pc=4 & k<N → 1 : (cte'=0) & (he'=2) & (pc'=0) &
(k'=k+1);
88
89 [] cte=1 & he=1 & a=0 & pc=4 & k<N → 1 : (cte'=3) & (pc'=0) & (k'=k+1);
90 [] cte=1 & he=1 & a=2 & pc=4 & k<N → 1 : (he'=0) & (pc'=0) & (k'=k+1);
91
92 [] cte=1 & he=2 & a=0 & pc=4 & k<N → 1 : (cte'=0) & (pc'=0) & (k'=k+1);
93 [] cte=1 & he=2 & a=1 & pc=4 & k<N → 1 : (he'=0) & (pc'=0) & (k'=k+1);
94
95 [] cte=3 & he=0 & a=0 & pc=4 & k<N → 1 : (pc'=0) & (k'=k+1);
96 [] cte=3 & he=0 & a=1 & pc=4 & k<N → 1 : (cte'=-1) & (pc'=5); //error
97 [] cte=3 & he=0 & a=2 & pc=4 & k<N → 1 : (cte'=1) & (he'=2) & (pc'=0) &
(k'=k+1);
98
99 [] cte=3 & he=1 & a=0 & pc=4 & k<N → 1 : (cte'=-1) & (pc'=5); //error
100 [] cte=3 & he=1 & a=2 & pc=4 & k<N → 1 : (he'=0) & (pc'=0) & (k'=k+1);
101
102 [] cte=3 & he=2 & a=0 & pc=4 & k<N → 1 : (cte'=1) & (pc'=0) & (k'=k+1);
103 [] cte=3 & he=2 & a=1 & pc=4 & k<N → 1 : (he'=0) & (pc'=0) & (k'=k+1);
104
105 // right-side dynamics:
106 [] cte=2 & he=0 & a=0 & pc=4 & k<N → 1 : (pc'=0) & (k'=k+1);
107 [] cte=2 & he=0 & a=1 & pc=4 & k<N → 1 : (cte'=0) & (he'=1) & (pc'=0) &
(k'=k+1);
108 [] cte=2 & he=0 & a=2 & pc=4 & k<N → 1 : (cte'=4) & (he'=2) & (pc'=0) &
(k'=k+1);
109
110 [] cte=2 & he=1 & a=0 & pc=4 & k<N → 1 : (cte'=0) & (pc'=0) & (k'=k+1);
111 [] cte=2 & he=1 & a=2 & pc=4 & k<N → 1 : (he'=0) & (pc'=0) & (k'=k+1);
112
113 [] cte=2 & he=2 & a=0 & pc=4 & k<N → 1 : (cte'=4) & (pc'=0) & (k'=k+1);
114 [] cte=2 & he=2 & a=1 & pc=4 & k<N → 1 : (he'=0) & (pc'=0) & (k'=k+1);
115
116 [] cte=4 & he=0 & a=0 & pc=4 & k<N → 1 : (pc'=0) & (k'=k+1);
117 [] cte=4 & he=0 & a=1 & pc=4 & k<N → 1 : (cte'=2) & (he'=1) & (pc'=0) &
(k'=k+1);
118 [] cte=4 & he=0 & a=2 & pc=4 & k<N → 1 : (cte'=-1) & (pc'=5); //error
119
120 [] cte=4 & he=1 & a=0 & pc=4 & k<N → 1 : (cte'=2) & (pc'=0) & (k'=k+1);
121 [] cte=4 & he=1 & a=2 & pc=4 & k<N → 1 : (he'=0) & (pc'=0) & (k'=k+1);
122

```

```

123     [] cte=4 & he=2 & a=0 & pc=4 & k<N → 1 : (cte'=-1) & (pc'=5); //error
124     [] cte=4 & he=2 & a=1 & pc=4 & k<N → 1 : (he'=0) & (pc'=0) & (k'=k+1);
125
126 endmodule

```

Listing 1.1: DTMC model without run-time guards

B.2 Model m_2 (with run-time guard)

```

1 dtmc
2
3 const N;
4 const M=10;
5
6 module taxinet
7
8     cte : [-1..4] init 0;
9     he : [-1..2] init 0;
10    v : [0..1] init 1;
11    cte_est : [0..4] init 0;
12    he_est : [0..2] init 0;
13    a : [0 .. 2] init 0;
14    pc : [0..5] init 0;
15    k : [1..N] init 1;
16
17    //number of sensor readings
18    i : [0..M] init 0;
19
20    // run-time guard based on Prophecy rules
21    [] pc=0 & i<M → 0.821: (v'=1) & (pc'=1) & (i'=0) +
22        0.179: (v'=0) & (i'=i+1); //repeat reading
23
24    // NN imperfect perception
25    [] cte=0 & v=1 & pc=1 → 0.909: (cte_est'=0) & (pc'=2) +
26        0.01: (cte_est'=1) & (pc'=2) +
27        0.081: (cte_est'=2) & (pc'=2) +
28        0.0: (cte_est'=3) & (pc'=2) +
29        0.0: (cte_est'=4) & (pc'=2);
30    [] cte=1 & v=1 & pc=1 → 0.556: (cte_est'=0) & (pc'=2) +
31        0.439: (cte_est'=1) & (pc'=2) +
32        0.0: (cte_est'=2) & (pc'=2) +
33        0.005: (cte_est'=3) & (pc'=2) +
34        0.0: (cte_est'=4) & (pc'=2);
35    [] cte=2 & v=1 & pc=1 → 0.369: (cte_est'=0) & (pc'=2) +
36        0.001: (cte_est'=1) & (pc'=2) +
37        0.628: (cte_est'=2) & (pc'=2) +
38        0.0: (cte_est'=3) & (pc'=2) +
39        0.002: (cte_est'=4) & (pc'=2);
40    [] cte=3 & v=1 & pc=1 → 0.315: (cte_est'=0) & (pc'=2) +
41        0.382: (cte_est'=1) & (pc'=2) +
42        0.0: (cte_est'=2) & (pc'=2) +
43        0.303: (cte_est'=3) & (pc'=2) +
44        0.0: (cte_est'=4) & (pc'=2);
45    [] cte=4 & v=1 & pc=1 → 0.232: (cte_est'=0) & (pc'=2) +
46        0.0: (cte_est'=1) & (pc'=2) +
47        0.346: (cte_est'=2) & (pc'=2) +
48        0.0: (cte_est'=3) & (pc'=2) +
49        0.422: (cte_est'=4) & (pc'=2);
50
51
52
53    [] he=0 & v=1 & pc=2 → 0.727: (he_est'=0) & (pc'=3) +
54        0.25: (he_est'=1) & (pc'=3) +
55        0.023: (he_est'=2) & (pc'=3);
56    [] he=1 & v=1 & pc=2 → 0.045: (he_est'=0) & (pc'=3) +
57        0.955: (he_est'=1) & (pc'=3) +
58        0: (he_est'=2) & (pc'=3);

```

```

59     [] he=2 & v=1 & pc=2 → 0.32: (he_est'=0) & (pc'=3) +
60         0.048: (he_est'=1) & (pc'=3) +
61         0.632: (he_est'=2) & (pc'=3);
62
63     // controller and airplane dynamics: same as before
64     ...
65 endmodule

```

Listing 1.2: DTMC model with run-time guards

C Parametric DTMC models for FACT

C.1 Model m_1 (no run-time guard; $v = 1$ always)

```

1  dtmc
2
3  const N=4;
4  param double p = 3440 604 40;
5  param double q = 1686 992 4 11;
6  param double r = 1119 4 2173 8;
7  param double t = 152 145 101;
8  param double h = 151 254 224;
9
10 param double x = 4748 2139 148;
11 param double y = 91 2010;
12 param double z = 744 211 1017;
13
14 module taxinet
15
16     cte : [-1..4] init 0;
17     he: [-1..2] init 0;
18     v: [0..1] init 1;
19     cte_est: [0..4] init 0;
20     he_est: [0..2] init 0;
21     a: [0 .. 2] init 0;
22     pc:[0..5] init 0;
23     k:[1..N] init 1;
24
25     [] pc=0 → 1: (v'=1) & (pc'=1);
26
27     [] cte=0 & v=1 & pc=1 → p1: (cte_est'=0) & (pc'=2) +
28         p2: (cte_est'=1) & (pc'=2) +
29         (1-p1-p2): (cte_est'=2) & (pc'=2);
30     [] cte=1 & v=1 & pc=1 → q1: (cte_est'=0) & (pc'=2) +
31         q2: (cte_est'=1) & (pc'=2) +
32         q3: (cte_est'=2) & (pc'=2) +
33         (1-q1-q2-q3): (cte_est'=3) & (pc'=2);
34     [] cte=2 & v=1 & pc=1 → r1: (cte_est'=0) & (pc'=2) +
35         r2: (cte_est'=1) & (pc'=2) +
36         r3: (cte_est'=2) & (pc'=2) +
37         (1-r1-r2-r3): (cte_est'=4) & (pc'=2);
38     [] cte=3 & v=1 & pc=1 → t1: (cte_est'=0) & (pc'=2) +
39         t2: (cte_est'=1) & (pc'=2) +
40         (1-t1-t2): (cte_est'=3) & (pc'=2);
41     [] cte=4 & v=1 & pc=1 → h1: (cte_est'=0) & (pc'=2) +
42         h2: (cte_est'=2) & (pc'=2) +
43         (1-h1-h2): (cte_est'=4) & (pc'=2);
44
45
46     [] he=0 & v=1 & pc=2 → x1: (he_est'=0) & (pc'=3) +
47         x2: (he_est'=1) & (pc'=3) +
48         (1-x1-x2): (he_est'=2) & (pc'=3);
49     [] he=1 & v=1 & pc=2 → y1: (he_est'=0) & (pc'=3) +
50         (1-y1): (he_est'=1) & (pc'=3);
51     [] he=2 & v=1 & pc=2 → z1: (he_est'=0) & (pc'=3) +
52         z2: (he_est'=1) & (pc'=3) +

```

```

53             (1-z1-z2): (he_est'=2) & (pc'=3);
54
55     // controller and airplane dynamics: same as before
56     ...
57
58 endmodule

```

Listing 1.3: Parametric DTMC model without run-time guards

C.2 Model m_2 (with run-time guard)

```

1  dtmc
2
3  const N=4;
4  const M=10;
5
6  param double c = 7496 1629;
7
8  param double p = 2984 32 259;
9  param double q = 1206 951 11;
10 param double r = 1069 2 1820 6;
11 param double t = 104 126 100;
12 param double h = 119 178 217;
13
14 param double x = 4025 1388 125;
15 param double y = 89 1902;
16 param double z = 512 76 1008;
17
18 module taxinet
19
20     cte : [-1..4] init 0;
21     he: [-1..2] init 0;
22     v: [0..1] init 1;
23     cte_est: [0..4] init 0;
24     he_est: [0..2] init 0;
25     a: [0 .. 2] init 0;
26     pc:[0..5] init 0;
27     k:[1..N] init 1;
28     i:[0..M] init 0;
29
30     [] pc=0 & i<M → c1: (v'=1) & (pc'=1) & (i'=0) +
31         (1-c1): (v'=0) & (i'=i+1); //repeat reading
32
33     [] cte=0 & v=1 & pc=1 → p1: (cte_est'=0) & (pc'=2) +
34         p2: (cte_est'=1) & (pc'=2) +
35         (1-p1-p2): (cte_est'=2) & (pc'=2);
36     [] cte=1 & v=1 & pc=1 → q1: (cte_est'=0) & (pc'=2) +
37         q2: (cte_est'=1) & (pc'=2) +
38         (1-q1-q2): (cte_est'=3) & (pc'=2);
39     [] cte=2 & v=1 & pc=1 → r1: (cte_est'=0) & (pc'=2) +
40         r2: (cte_est'=1) & (pc'=2) +
41         r3: (cte_est'=2) & (pc'=2) +
42         (1-r1-r2-r3): (cte_est'=4) & (pc'=2);
43     [] cte=3 & v=1 & pc=1 → t1: (cte_est'=0) & (pc'=2) +
44         t2: (cte_est'=1) & (pc'=2) +
45         (1-t1-t2): (cte_est'=3) & (pc'=2);
46     [] cte=4 & v=1 & pc=1 → h1: (cte_est'=0) & (pc'=2) +
47         h2: (cte_est'=2) & (pc'=2) +
48         (1-h1-h2): (cte_est'=4) & (pc'=2);
49
50
51     [] he=0 & v=1 & pc=2 → x1: (he_est'=0) & (pc'=3) +
52         x2: (he_est'=1) & (pc'=3) +
53         (1-x1-x2): (he_est'=2) & (pc'=3);
54     [] he=1 & v=1 & pc=2 → y1: (he_est'=0) & (pc'=3) +
55         (1-y1): (he_est'=1) & (pc'=3);
56     [] he=2 & v=1 & pc=2 → z1: (he_est'=0) & (pc'=3) +

```

```

57         z2: (he_est'=1) & (pc'=3) +
58         (1-z1-z2): (he_est'=2) & (pc'=3);
59
60     // controller and airplane dynamics: same as before
61     ...
62
63 endmodule

```

Listing 1.4: Parametric DTMC model with run-time guards

D Rules Mined from TaxiNet as Run-time Guards

In previous work [31] we explored the use of rules mined from the TaxiNet model for the purpose of *explaining* correct and incorrect model behavior. The rules are in the form of $Pre \implies Post$, where the Pre condition is in terms of neuron constraints in the latent space of the network and characterizes inputs on which the $Post$ condition (property of the network outputs) is satisfied. The following correctness property of the regression outputs was considered in [31], $|cte^* - cte| \leq 1.0 \text{ meters} \wedge |he^* - he| \leq 5 \text{ degrees}$, and rules for the satisfaction and violation of this property were extracted. We used the Prophecy tool [16] to extract these rules. Given a set of inputs, the tool builds a set comprising of the neuron values corresponding to each input and a label of whether the $Post$ was satisfied or not, which in turn is fed to decision-tree learning. There could be more than 1 rules per label, each of which has 100% precision on the input set and a metric of support representing the number of inputs satisfying the neuron constraints in the corresponding pre-condition.

Leveraging this work, we extracted rules for valid and invalid behavior of the Taxinet regression model using a separate set of 5554 test inputs. The rules were extracted using the neurons from the three dense layers of the network (dense_1 layer with 100, dense_2 with 50 and dense_3 with 10 neurons respectively). Example of a rule for invalid behavior:

$$\begin{aligned}
 & N_{1,85} \leq -0.998 \wedge N_{2,50} \leq 3.31 \wedge N_{1,84} \leq -0.994 \wedge N_{1,15} > -0.999 \\
 & \wedge N_{1,21} \leq 1.711 \wedge N_{1,70} \leq 11.088 \wedge N_{1,51} > -0.999 \wedge N_{1,21} > -0.637 \implies \\
 & |cte^* - cte| > 1.0 \text{ meters} \vee |he^* - he| > 5 \text{ degrees}
 \end{aligned}$$

Here $N_{i,j}$ indicates the j^{th} neuron in the i^{th} dense layer. This rule has a support of 755, indicating that 755 (out of 5554) inputs satisfied the neuron constraints specified in Pre and the DNN violated the correctness property for each of them.

For our case study, we experimented with deploying the rules for invalid behavior as run-time guards to catch inputs potentially leading to misbehavior. In order to obtain good coverage while maintaining high precision, we selected rules with the support greater than a threshold. When running on the dataset with 11108 inputs, inputs that satisfied any of the selected rules were discarded (1983 inputs), thereby abstaining the model from potential misbehavior. The regression model behavior improved (MAE for cte : 1.07, MAE for he : 6.39), which in turn improved the accuracies on the classification abstraction as well

(**cte**: 65.78%, **he**:76%). The new confusion matrix (computed for the inputs that pass the run-time guard) and transition probabilities are shown in Table 3. While we use rules for invalid behavior for the purpose of this demonstration, we could also employ other run-time guards using e.g., the rules for valid behavior, or rules for correct/incorrect behavior wrt. the discretized outputs and easily integrate them in our approach.

E Limitations of FACT

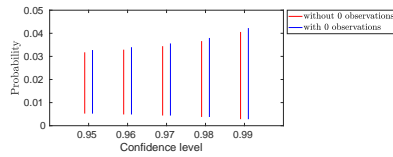


Fig. 5: Confidence interval results for m_1 , Property 2, $N = 3$.

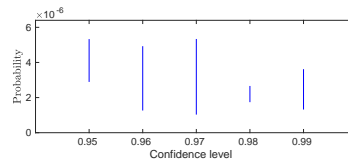


Fig. 6: Confidence interval results for m_2 , $N = 4$

We discuss here some hurdles we encountered with the application of FACT.

Scalability. Technically, even for a DTMC transition that has zero probability mass due to zero observations in the data, for the purpose of confidence analysis, we should add a parameter to the model representing the probability of the transition (and specify the number of observations as zero). However, we found this approach scales poorly. For instance, for model m_1 and Property 2 (which is the easiest to analyze), we could not obtain results beyond $N = 3$ with FACT and we could not obtain any results for the other properties or for m_2 .

In contrast, if we remove the transitions with zero observations, the model has fewer parameters and the analysis scales better. For instance, on a Windows OS machine with 11th Gen Intel(R) Core(TM) i7 processor and 64GB RAM, FACT finishes in 5.783s (model without zero-observations transitions) vs. 140.676s (model with zero-observations transitions).

Figure 5 shows the results obtained for m_1 with and without modeling transitions with zero observations. As the difference between computed intervals is very small, we have decided to report in this paper on the analysis for models with those transitions removed (for which we could obtain results for $N = 4$). Note that whether these transitions are included or not has no effect on the results of the PRISM analysis. Also note that one could attempt to prove the absence of such transitions (using DNN-specific analysis) obtaining as a result an abstraction that is more amenable to verification.

Scalability issues in FACT arise due to the complexity of the computational problems solved by FACT in each of its two stages. In the first stage, FACT uses *parametric model checking* to generate an algebraic expression (for the probability of the property ϕ under analysis) which is a multivariate rational function that depends on the unknown transition probabilities. This stage can lead to scalability

issues due to state explosion during parametric model checking. In the second stage, referred to *confidence interval inference*, FACT uses the observations to derive confidence intervals for each unknown transition probability appearing in the algebraic expression and then uses them to derive the required confidence interval for ϕ ; the analysis is based on the concept of simultaneous confidence intervals for a multinomial distribution and requires solving optimization problems. The second stage can give rise to scalability issues due the complexity of the optimization problems to be solved. Newer work [12] promises to scale much better, however we have found it not mature enough to be applicable to our models. We are working on improving the tool for future use.

Numerical Issues. We conducted confidence analysis for *Property 3* on model m_2 , for $N = 4$, without the zero-observations transitions. Figure 6 shows the calculated confidence intervals for the probability of satisfying the property at different confidence levels. One would expect, (i) the intervals to get larger for higher confidence levels; (ii) the intervals at higher confidence levels to include the ones at lower levels. However, the probabilities for *Property 3* are very small (on the order of $1e-6$). We suspect that the Gurobi Optimizer [21] (which FACT uses internally at the confidence interval inference stage) is unable to handle the problem of finding the minima and maxima corresponding to the confidence interval bounds for such small probabilities, and as a consequence, we see confidence intervals that do not grow monotonically in size with the confidence levels. Additionally, the confidence intervals being calculated are meant to be conservative. As such, having non-monotonically growing intervals with increasing confidence levels is not necessarily wrong. It may only mean that the analysis engine could not do any better, and the intervals at lower confidence levels are over-conservative.